

# We are IntechOpen, the world's leading publisher of Open Access books Built by scientists, for scientists

6,900

Open access books available

186,000

International authors and editors

200M

Downloads

Our authors are among the

154

Countries delivered to

TOP 1%

most cited scientists

12.2%

Contributors from top 500 universities



WEB OF SCIENCE™

Selection of our books indexed in the Book Citation Index  
in Web of Science™ Core Collection (BKCI)

Interested in publishing with us?  
Contact [book.department@intechopen.com](mailto:book.department@intechopen.com)

Numbers displayed above are based on latest data collected.  
For more information visit [www.intechopen.com](http://www.intechopen.com)



---

# Tungsten Carbide as an Reinforcement in Structural Oxide-Matrix Composites

---

Zbigniew Pędzich

Additional information is available at the end of the chapter

<http://dx.doi.org/10.5772/51183>

---

## 1. Introduction

The possibility of serious improvement of mechanical properties of oxide ceramics by particulate composites manufacturing has been recently recognized very well. Among oxide ceramics, tetragonal zirconia solid solutions and  $\alpha$ -alumina phase are the most important materials, widely used in structural applications, due to their good properties. The fabrication of two-phase particulate composites could be the simplest way to the mechanical properties improvement. Despite a wide range of alumina-zirconia composites, non-oxide particles were also often utilized as strengthening agents. Many phases were introduced into zirconia and alumina matrices - TiC, SiC, WC, TiB<sub>2</sub>, TiN, AlN, (Ti,W)C, Cr<sub>2</sub>O<sub>3</sub>, Cr<sub>7</sub>C<sub>3</sub>, and metals - nickel, molybdenum and tungsten and others [1-17]. In this way, the materials with improved properties, when compared with “pure” matrix materials, were obtained. Depending on the type of inclusions, their size and amount as well as sintering conditions, one can achieve a significant improvement of hardness, stiffness, fracture toughness and/or strength of the material. It was also reported that the decrease of inclusion size to the nanometric scale allowed extremely high values of flexural strength and fracture toughness to be achieved.

The manufacturing of composites with ceramic matrix almost always leads to residual stresses caused by the mismatch of thermal properties of constituent phases. A large difference in thermal expansion coefficients (CTE's) could introduce stresses reaching even more than gigaPascals to the composite system. Such a phenomenon has to influence the way of fracture and consequently the strength and the fracture toughness of the material. The value of these stresses mainly depends on mechanical properties of constituent phases of the composite and the absolute difference between their CTE's. The distribution of residual stresses depends also on the phase arrangement and shape of grains. This chapter presents the investigation results on the influence of the phase arrangement on the way of

fracture in composites. These observations were put together with the results of mechanical properties measurements and abrasive wear tests.

## 2. Thermodynamical aspect

### 2.1. ZrO<sub>2</sub>/WC system

Zirconia for structural applications is used in the form of solid solutions of yttria, magnesia, calcia or rare earth metals in ZrO<sub>2</sub> [18-20]. Using data from [21] one can calculate that free enthalpy of mixing of zirconia and any stabilizing element is significantly lower than the error of determination of free enthalpy for chemical reactions in ZrO<sub>2</sub>-WC (or ZrO<sub>2</sub>-WC-C) systems. It allows to calculate, with a reasonable approximation, the possibility of reactions proceeding using thermo-dynamical data for zirconia only.

Potential chemical reactions taken into account were as follow:



Calculations showed that reaction (1) cannot proceed in the range of potential sintering temperatures (1400 - 1700°C) because of fact that standard free enthalpy ( $\Delta G_r^0$ ) of that reaction is much higher than zero.

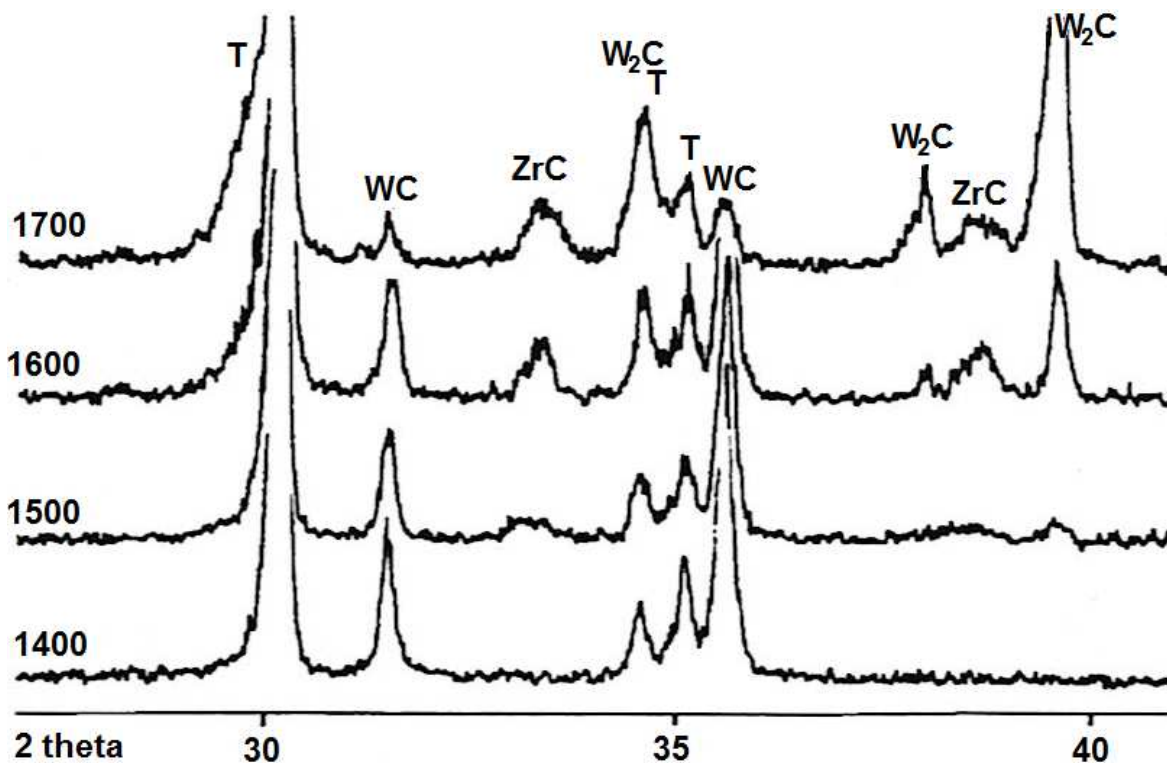


**Figure 1.** Results of XRD analyses of 3Y-ZrO<sub>2</sub>/10vol.% of WC composite pressureless sintered at different temperatures. T: stand for tetragonal phase of the zirconia solid solution, sintering temperatures indicated on the left side of plots.

Reaction (2) can proceed when the partial pressure of CO in the system is lower than 0.95 atm at 1400°C, 5.20 atm at 1500°C, 23.8 atm at 1700°C and 93.0 atm at 1700°C.

These calculations were verified experimentally [22]. The presence of ZrC and W<sub>2</sub>C was determined in sinters containing WC inclusions sintered at different temperatures (Fig. 1.).

If sintering process is conducted using hot-pressing (HP) technique, composite powder could be in contact with carbon from the press die or stamps. It suggest that the third reaction should be also taken into account:



Reaction (3) can proceed when the partial pressure of CO in the system is lower than 0.054 atm at 1400°C, 0.20 atm at 1500°C, 0.65 atm at 1700°C and 1.89 atm at 1700°C. These data suggest that is possible to produce ZrC precipitates even in pure zirconia sinters when one can assure right value of CO pressure [17]. Conducting of sintering process at relatively low temperature (1400°C ) allows to avoid ZrC appearance (Fig. 2).

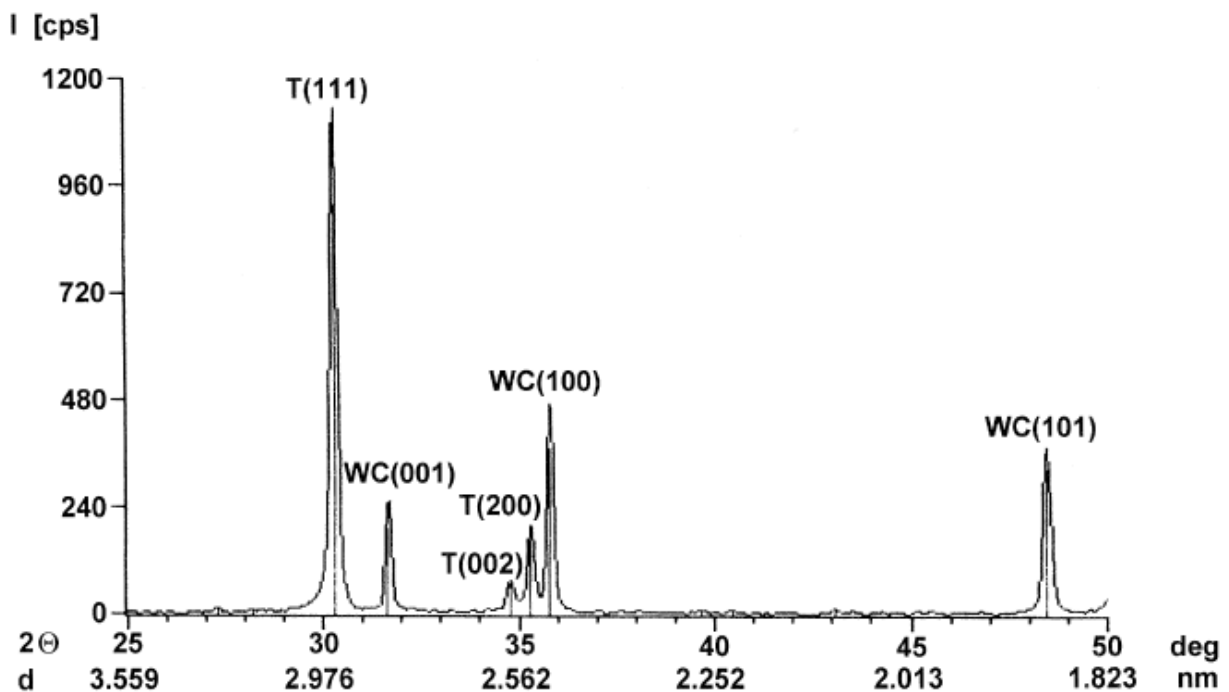
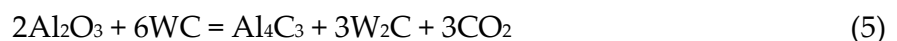


**Figure 2.** Result of XRD analysis of 3Y-ZrO<sub>2</sub>/10vol.% of WC composite hot-pressed at 1500°C. T: stand for tetragonal phase of the zirconia solid solution.

## 2.2. Al<sub>2</sub>O<sub>3</sub>/WC system

Potential chemical reactions in alumina – tungsten carbide systems taken into account:





Calculations showed that reactions (4 - 6) cannot proceed in the range of potential sintering temperatures (1400 - 1700°C) because of fact that standard free enthalpy ( $\Delta G_r^0$ ) of that reaction is much higher than zero. That results were also confirm by Niyomwas [23], who stated that  $\text{Al}_2\text{O}_3/\text{WC}$  system is thermodynamically stable up to 2000°C.

### 3. Internal stress state

The manufacturing of composites with ceramic matrix almost always leads to residual stresses caused by the mismatch of thermal properties of constituent phases. The value of these stresses mainly depends on mechanical properties of constituent phases of the composite and the absolute difference between their CTE's. A large difference in thermal expansion coefficients (CTE's) could introduce to the composite system stresses reaching even more than gigaPascals. Such a phenomenon has to influence mechanical properties of the material. The distribution of residual stresses depends also on the phase arrangement and shape of grains.

Phase	CTE ( $\alpha$ ), $\cdot 10^{-6}\text{C}^{-1}$	Young modulus $E$ , GPa	Poisson ratio, $\nu$
Alumina	7.9	385	0.250
Zirconia ss.	11.0	210	0.210
WC	5.2	700	0.300

**Table 1.** Data necessary for calculation of the residual stresses value.

The thermal expansion coefficient of tungsten carbide ( $\alpha_{\text{WC}}$ ) is lower than thermal expansion coefficients of both considered oxide phases ( $\alpha_{\text{Al}_2\text{O}_3}$  and  $\alpha_{\text{ZrO}_2}$ ). It means that in composites with both oxide matrices the internal stress state is similar. Matrices are under tension and carbide inclusions are under compression.

For this chapter results of calculation of stresses in materials was made using the finite elements model (FEM) based on following predictions:

- the grain in the matrix in two-dimensional geometry,
- the model was constrained to enable a free deformation in  $xy$  plane to be carried out and, additionally, in one corner,
- the geometric model was discretized with the AutoGEM modulus [24, 25]. For calculations the elements neighboring the point of support were excluded. This eliminated the stress accumulation at the model edge,
- grain boundaries inside constituent phases were omitted,
- calculations were made using the mechanical property values (Young's moduli, Poisson ratio's and CTE's) placed in Table 1. Isotropy of these constants was taken as a principle,
- modeling was performed for the plain stress state,
- Used method of load was cooling from temperature of 1200°C to room temperature

The results of FEM simulations were visualized at Figures 3 and 4. They present the distribution of principal maximal stresses around in the hypothetical composite microstructure. Calculations were made for the same schematic microstructure. Matrix was assumed as zirconia or alumina, respectively. The inclusion phase was WC. Calculations were made for  $\text{Al}_2\text{O}_3/\text{WC}$  and  $\text{ZrO}_2/\text{WC}$  composites.

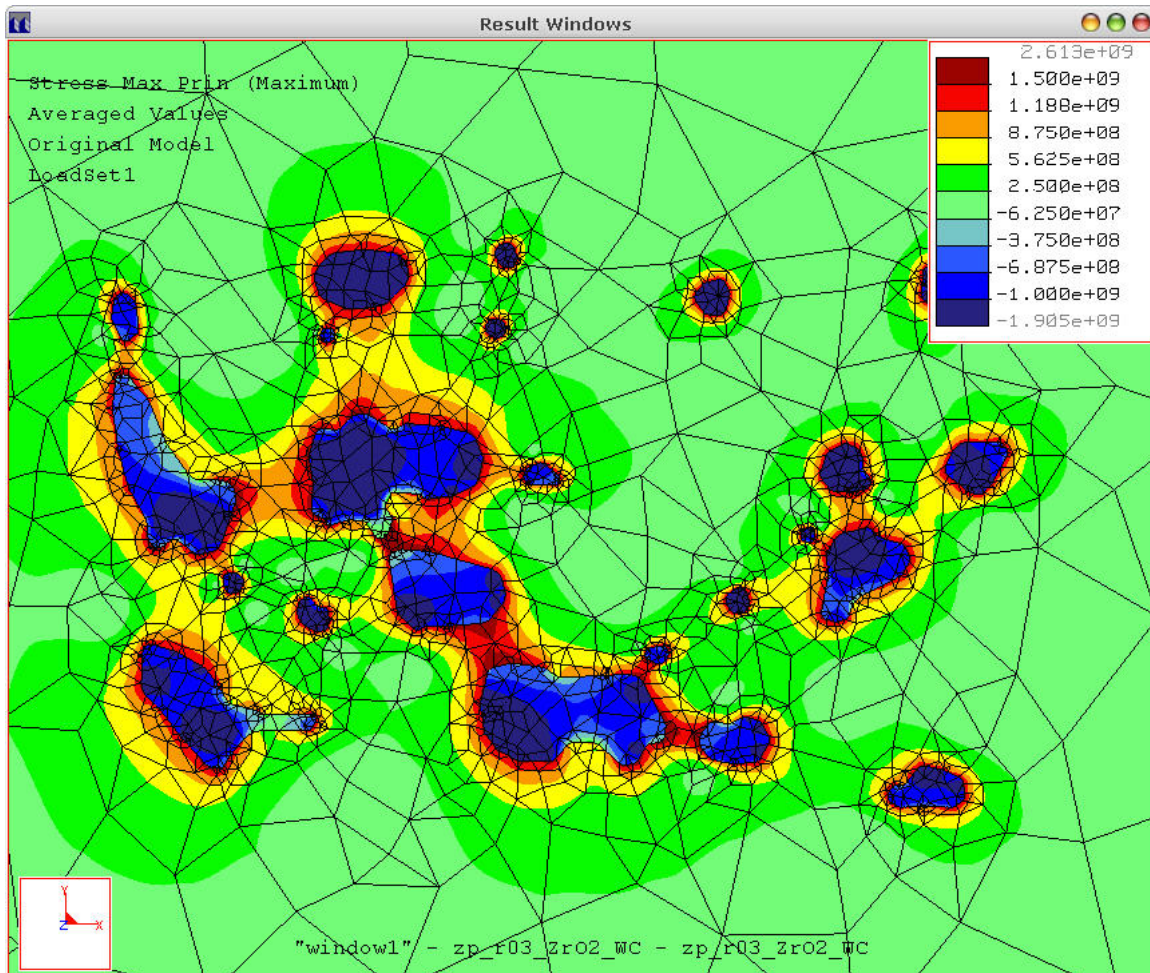


**Figure 3.** The principal maximal stresses calculated for  $\text{ZrO}_2/\text{WC}$  composite. Dark blue color represents the maximal values of compressive stresses, brown color represents the maximal values of tensile stresses. At this Figure WC inclusions are generally in blue color.

Generally, the maximum value of principal maximal stresses in the zirconia matrix is about 30 % higher than in the alumina one. The tensile stress level near the interphase boundary in the zirconia matrix materials exceeds 1000 MPa all around the inclusion grain (Fig. 3). In the alumina based materials maximum stress values in this area are much lower (Fig. 4).

This fact influences the path of crack in the investigated materials. In zirconia-based composites crack goes along the interphase boundary (Fig. 5). The crack course in composites with alumina matrix is different. It usually goes near the inclusion grains, but it is deflected before it reaches the interphase boundary (Fig. 6). This means that the crack goes through alumina grains.

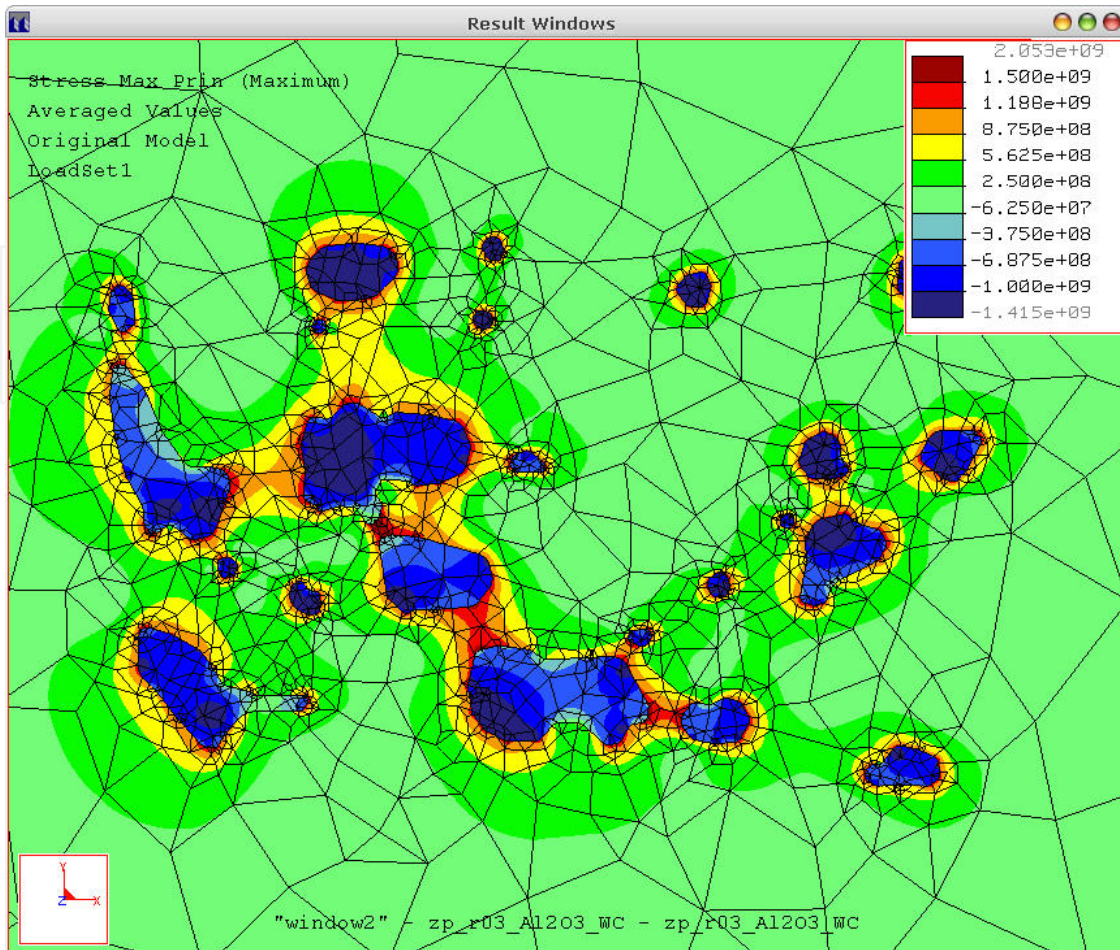


**Figure 4.** The principal maximal stresses calculated for  $\text{Al}_2\text{O}_3/\text{WC}$  composite. Dark blue color represents the maximal values of compressive stresses, brown color represents the maximal values of tensile stresses. At this Figure WC inclusions are generally in blue color.

The final effect of such crack behaviour for material toughening is summarized in Table 4. As it is clearly visible, the relative fracture toughness increase observed for the alumina-based composites is higher than for the zirconia ones.

This phenomenon should be attributed to the lower stress level in the alumina-based composites. As it can be seen at Figures 3 – 4, the maximum stress values are present in some distance between inclusion grains. Probably the strength of alumina grain is comparable with the strength of interphase boundaries ( $\text{Al}_2\text{O}_3/\text{WC}$ ) in composites. Such a situation promotes transgranular cracking of alumina (see Fig. 6), but in a specific way, the crack still wanders around inclusions and crack deflection mechanism is still active and it consumes energy effectively.

In TZP matrix composites the tensile stress acting on the interphase boundary is much higher than in these with alumina matrix. It decrease the amount of energy dissipated during cracking. Additionally, high toughness of the zirconia material causes that the crack does not deflect as in the case of alumina. The crack rather goes to the interphase boundary and deflects directly on it. These observations are only qualitative but they could help to understand the effect of a relatively high level of toughening in the alumina based composites.

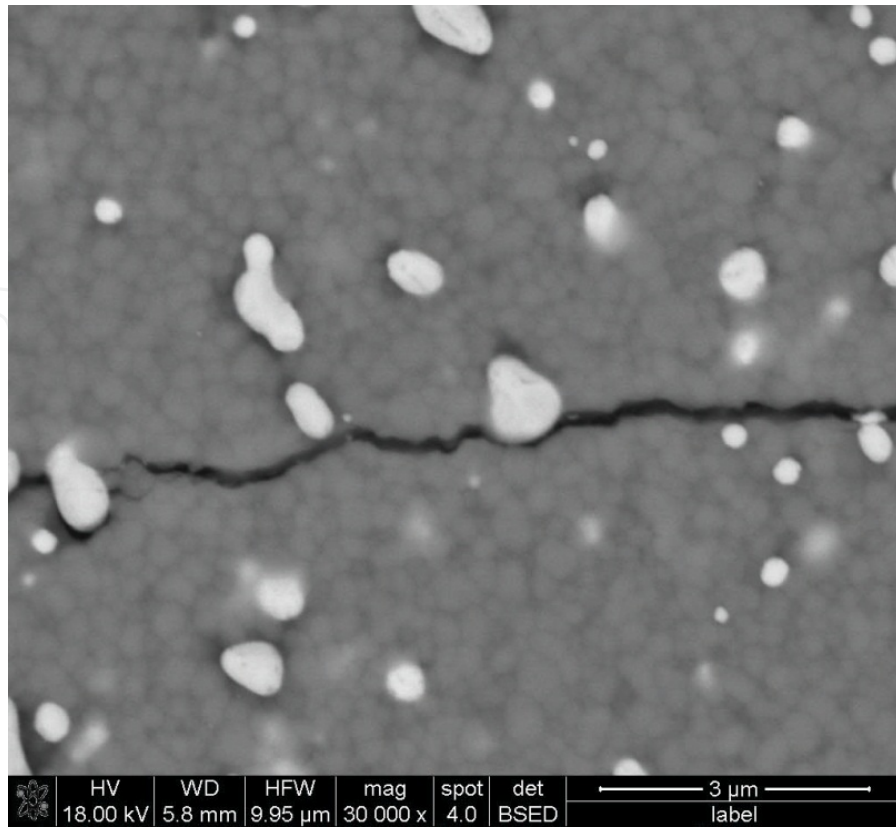


**Figure 5.** The SEM image of crack path in  $ZrO_2/WC$  composite.

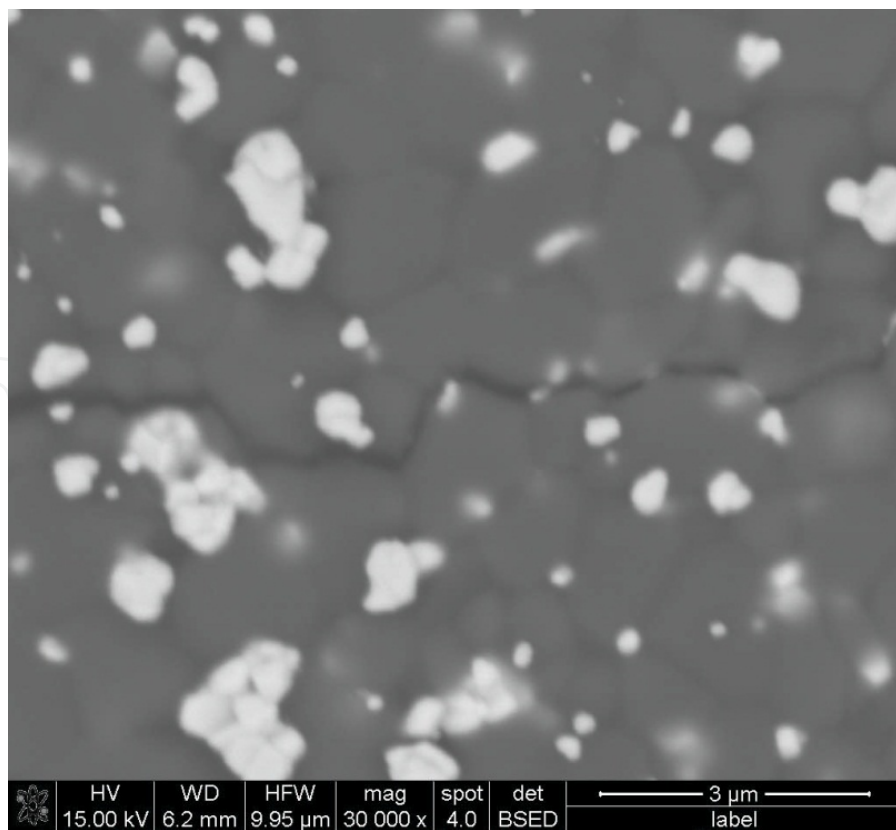


**Figure 6.** The SEM image of crack path in  $Al_2O_3/WC$  composite.

#### 4. Composite manufacturing

Preparation of dense particulate composite bodies with randomly distributed inclusions meets potential difficulties during composite powder preparation and during sintering. The most popular method of second phase dispersion in the matrix is simple mixing. This method is widely used for zirconia/WC system [26-28]. The mixing process utilizing intensive mills (attritors, rotation-vibrational mills) in short time assures the proper tungsten carbide particles distribution within the matrix in the wide range of WC content 10 – 50 vol. %. More sophisticated methods as for instance decomposition of organic WC precursors are nowadays too expensive for wider application [23, 29, 30].

In alumina/WC composite system the mechanical mixing is also the main preparation method of the composite powder. Anyway, there were some experiments [23] utilizing self-propagating high temperature synthesis (SHS) process for *in-situ* synthesis of alumina/tungsten carbide composite powder. In this process both tungsten carbides (WC, W<sub>2</sub>C) were present in the product.

Sintering of composites with oxide matrices and dispersed WC particles is a typical example of sintering with “rigid inclusions” widely described in literature [31-33]. In fact, during this process, diffusional mechanisms of densifications appear only in the oxide matrix. The presence of carbide particles makes the sintering driving forces much weaker. This effect is as stronger as higher is tungsten carbide particles volume content. The high relative density demand for structural applications (> 97 % of theo.) can be assured using pressureless sintering method when WC content not exceed 20 vol. %. Additionally, sintering temperature in this case must be relatively high (1550°C for zirconia and 1600°C for alumina). It is not profitable for sinters microstructure because the grain growth phenomenon. The inert sintering atmosphere demanded for preservation of WC from oxidation at high temperatures causes some additional factor of stabilization in zirconia [22, 34].

Practically, the most often sintering method for both type of composites is hot-pressing technique. Application of this method allows to assure high densities (> 98 % of theo.) in relatively short time (30 – 60 min.). Such conditions limits the grain growth in the matrix (see Table 3).

There were some investigations utilizing pulsed electric current sintering (PECS) for zirconia/WC composite densification [27]. These methods were profitable when WC content in the composite was relatively high (~30-40 vol. %).

#### 5. Composites microstructure

In present chapter author was focused on properties of “classical” particulate composites. It means materials containing the second phase particles randomly distributed into matrix. It means that the amount of additives must be lower than a percolation threshold. To assure that situation examples of composite materials contain 10 vol. % of tungsten phase with the same grain size distribution were manufactured.

Commercial powders were used as a starting materials (alumina – TM-DAR Taimicron, zirconia – Tosoh 3Y-TZ, tungsten carbide – Baildonit). Powders homogeneity was assured by 30 min. of attrition mixing of constituent powders in ethyl alcohol.

Materials for test were fabricated by hot-pressing technique (HP) due to guarantee the maximum of the densification of investigated samples. The sintering conditions were as follow: the maximum temperature - 1500°C (for zirconia and zirconia/WC composite) and 1650°C (for alumina and alumina/WC composite) with 1 hour soaking time and maximum applied pressure - 25 MPa.

A typical SEM microstructures of hot-pressed composites were showed in the Figs. 7 and 8. Table 2 collects data about the grain size of individual phases.

Material	Mean grain size, $\mu\text{m}$		
	$\text{Al}_2\text{O}_3$	$\text{ZrO}_2$	WC
Alumina	$5.20 \pm 2.90$	-	-
Alumina/10vol.% WC	$1.25 \pm 0.80$	-	$0.45 \pm 0.30$
Zirconia solid solution	-	$0.32 \pm 0.18$	-
Zirconia/10vol.% WC	-	$0.27 \pm 0.15$	$0.47 \pm 0.35$

**Table 2.** The mean grain size of phases existing in sinters containing 10 vol. % of WC.

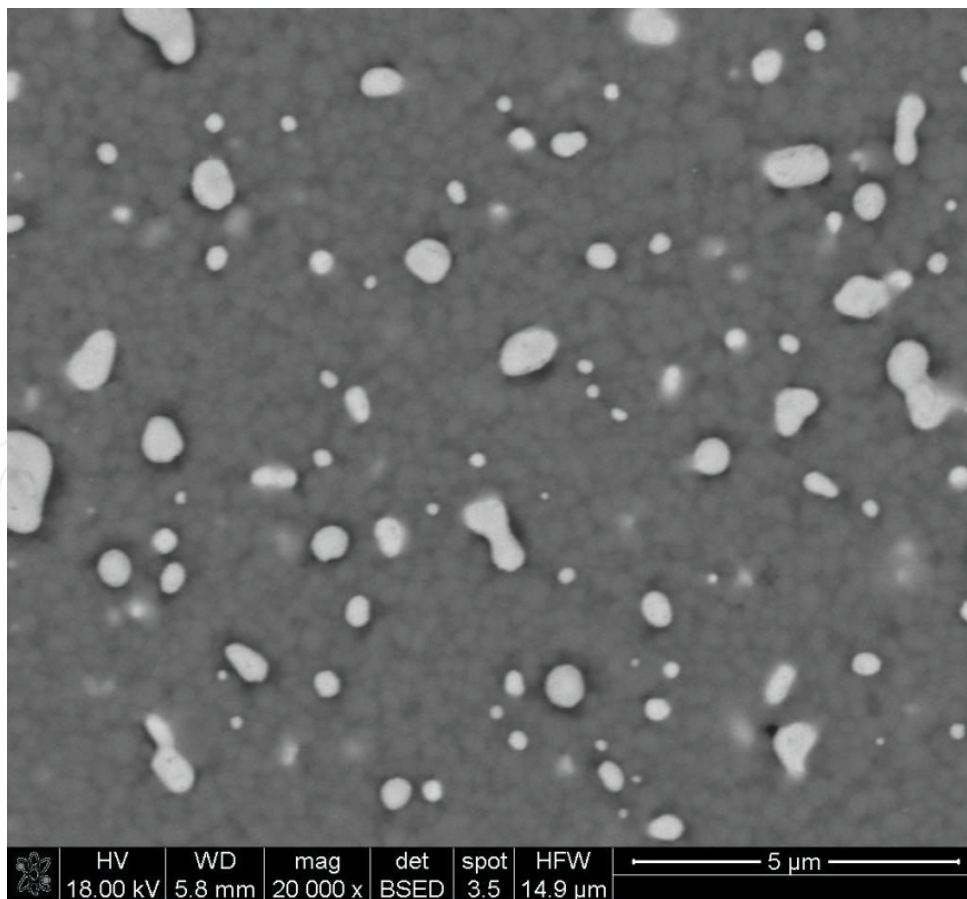


**Figure 7.** The typical SEM image of thermally etched  $\text{ZrO}_2/\text{WC}$  composite microstructure.

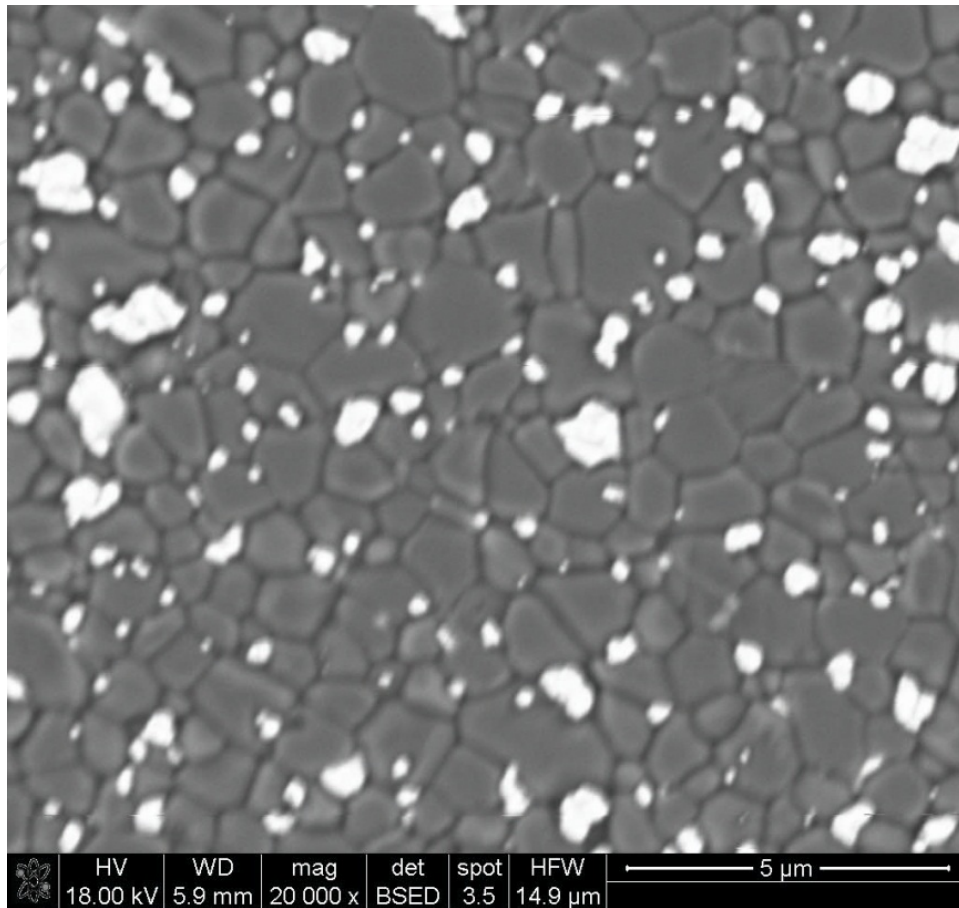


**Figure 8.** The typical SEM image of thermally etched  $\text{Al}_2\text{O}_3/\text{WC}$  composite microstructure.

Measurements performed in the TEM revealed that oxide matrices and tungsten carbide grains close adhered and no discontinuities were observed (Figs. 9 and 10).

The detail observation of  $\text{Al}_2\text{O}_3/\text{WC}$  and  $\text{ZrO}_2/\text{WC}$  microstructures and chemical analyses performed as a line scan across the interphase boundaries (Figs. 11 and 12) showed that there are differences in elements diffusion in investigated systems. The change of chemical composition near alumina/tungsten carbide boundary is sharp and distinct (Fig. 9). There is no evidence of Al diffusion into WC or W diffusion into  $\text{Al}_2\text{O}_3$ . In the case of zirconia/tungsten carbide boundary chemical composition is changing near the interphase boundary. It could be a slight confirmation of thermo-dynamically described tendency to creation of  $\text{ZrC}$  and  $\text{W}_2\text{C}$  in this system.

Results of TEM investigations have shown specific crystallographic relationships between alumina and zirconia matrix and tungsten carbide phase [35]. Crystal correlations may partially explain significant improvement of mechanical properties of alumina- and zirconia-based composites comparing with a pure oxide matrices. However, apart from crystallographic factors, the properties of material under investigation may be affected by interfacial defects and interphase boundary structure.

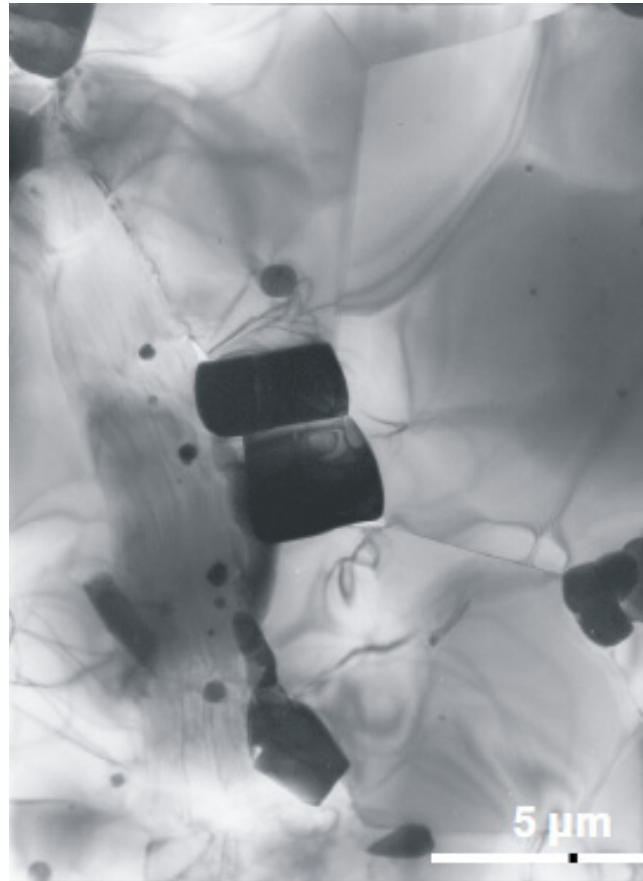


**Figure 9.** TEM micrograph of Al<sub>2</sub>O<sub>3</sub>/WC composite. Dark grains – WC; bright ones – alumina.

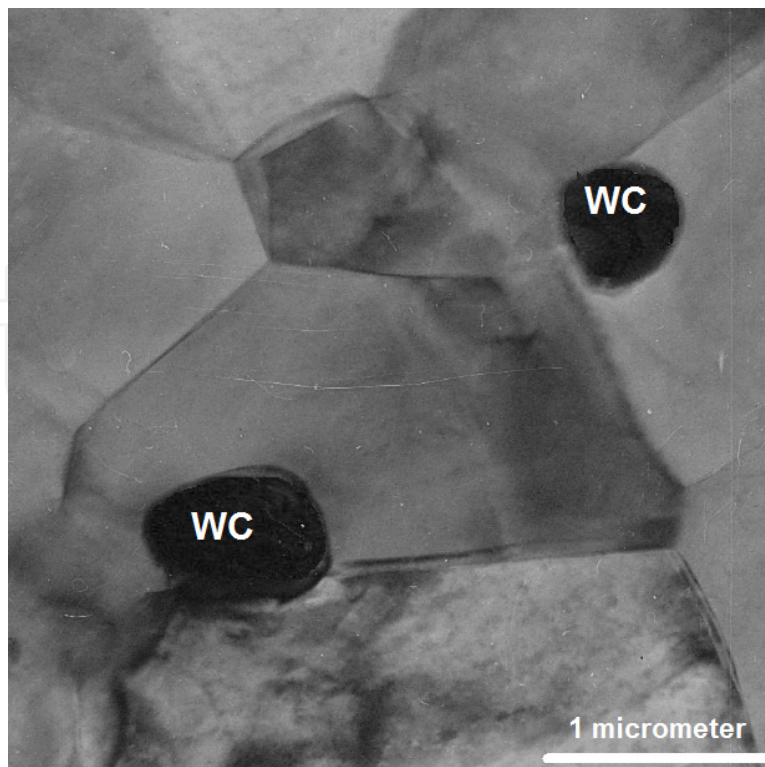


**Figure 10.** TEM micrograph of ZrO<sub>2</sub>/WC composite.

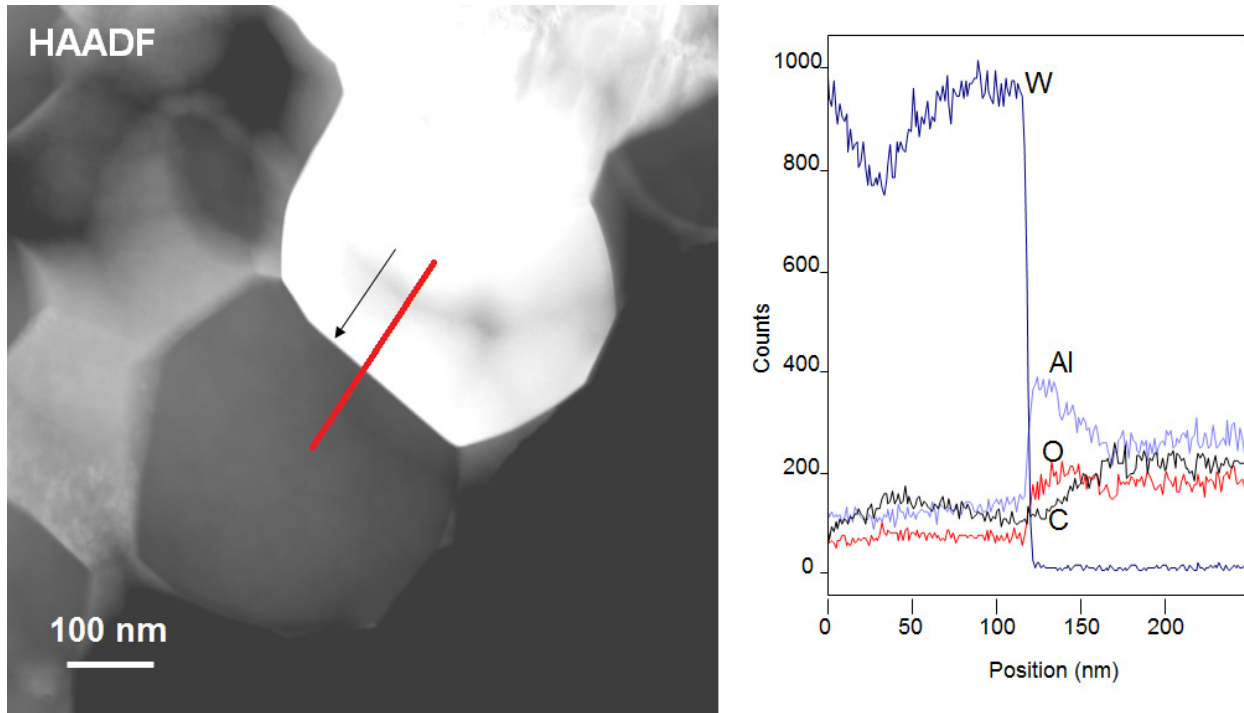


**Figure 11.** High resolution TEM microstructure of Al<sub>2</sub>O<sub>3</sub>/WC and the line scan across alumina and tungsten carbide boundary.

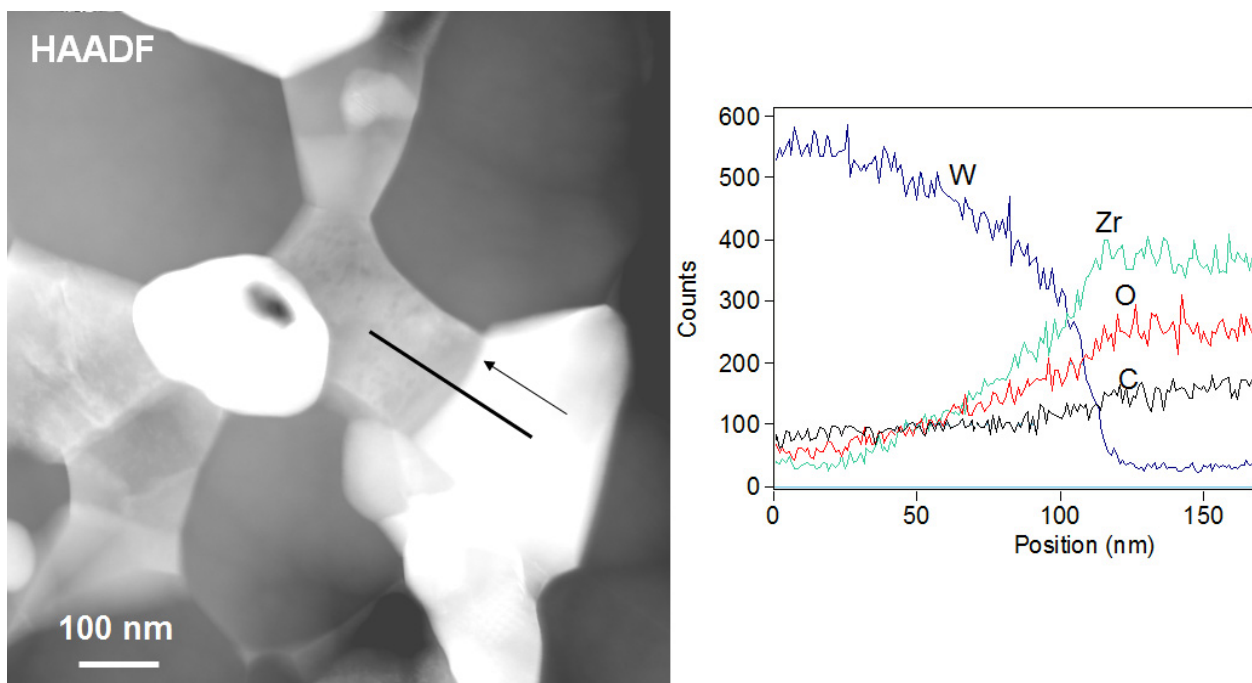


**Figure 12.** High resolution TEM microstructure of ZrO<sub>2</sub>/WC and the line scan across zirconia and tungsten carbide boundary.

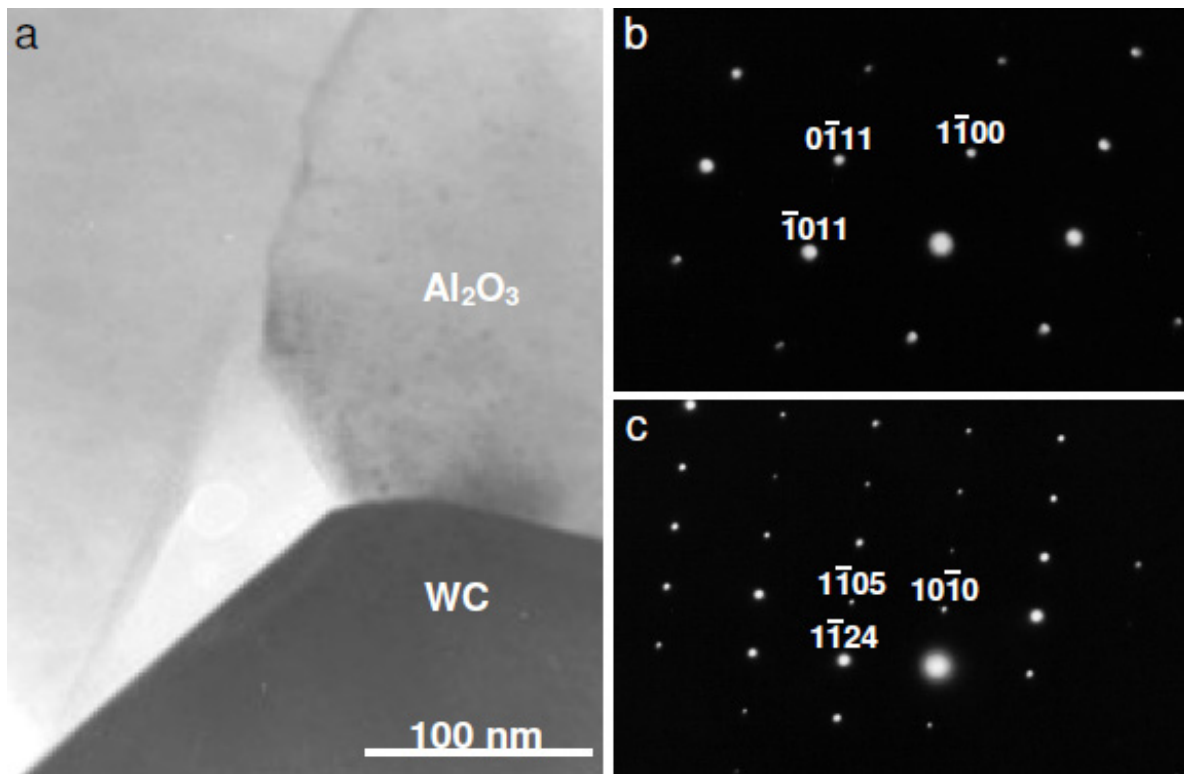


**Figure 13.** TEM micrograph of  $\text{Al}_2\text{O}_3/\text{WC}$  composite. a – bright field (BF) image, b – selected area electron diffraction (SEAD) from WC grain, c - SEAD from  $\text{Al}_2\text{O}_3$  grain.

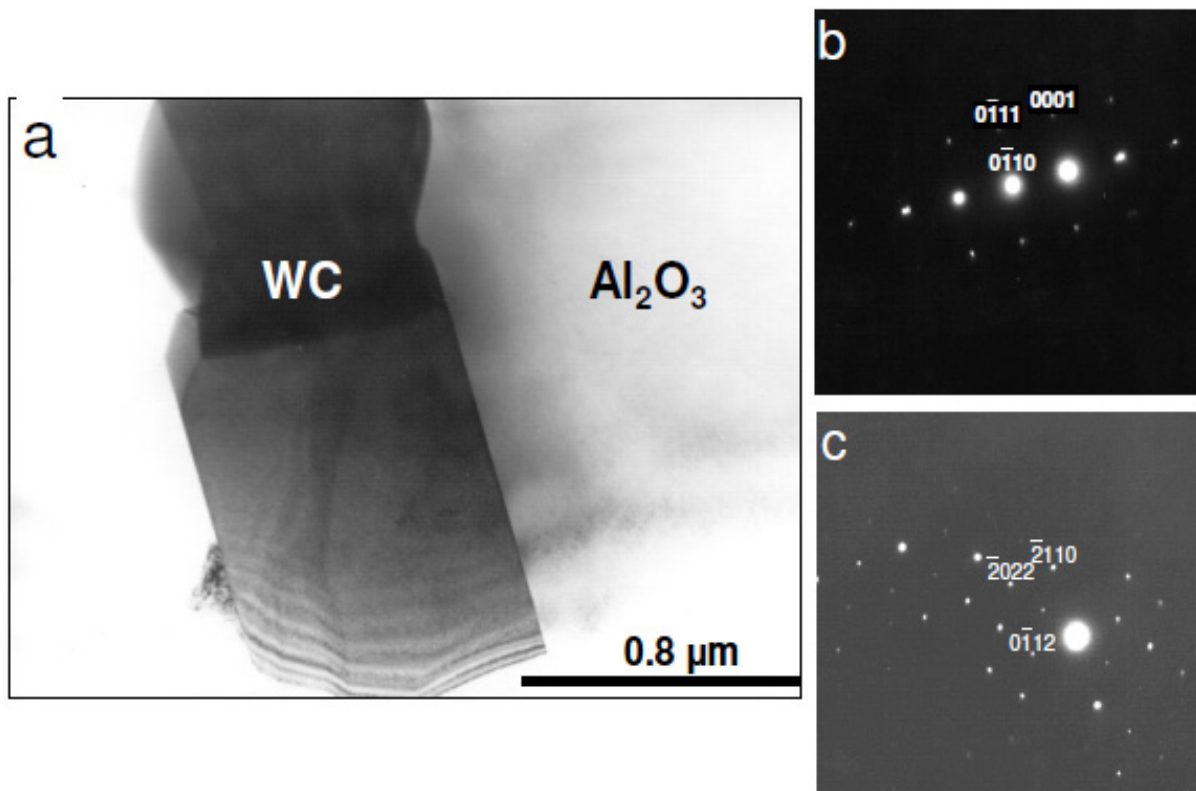


**Figure 14.** TEM micrograph of  $\text{Al}_2\text{O}_3/\text{WC}$  composite. a – BF image, b –SEAD from WC grain, c - SEAD from  $\text{Al}_2\text{O}_3$  grain.

Alumina and WC grains were indexed using the SAED “(Selected Area Electron Diffraction) and two characteristic crystal relationships between above phases were identified (Figs. 13 and 14):

$$(0\ 111)\ \text{WC} \parallel (1\ 105)\ \text{Al}_2\text{O}_3 \quad (7)$$

$$[11\ 23]\ \text{WC} \parallel [23\ 11]\ \text{Al}_2\text{O}_3 \quad (8)$$

and

$$(0\ 111)\ \text{WC} \parallel (1011)\ \text{Al}_2\text{O}_3 \quad (9)$$

$$[2\ 1\ 10]\ \text{WC} \parallel [01\ 11]\ \text{Al}_2\text{O}_3 \quad (10)$$

These relationships were found on several sites investigated on the thin foil.

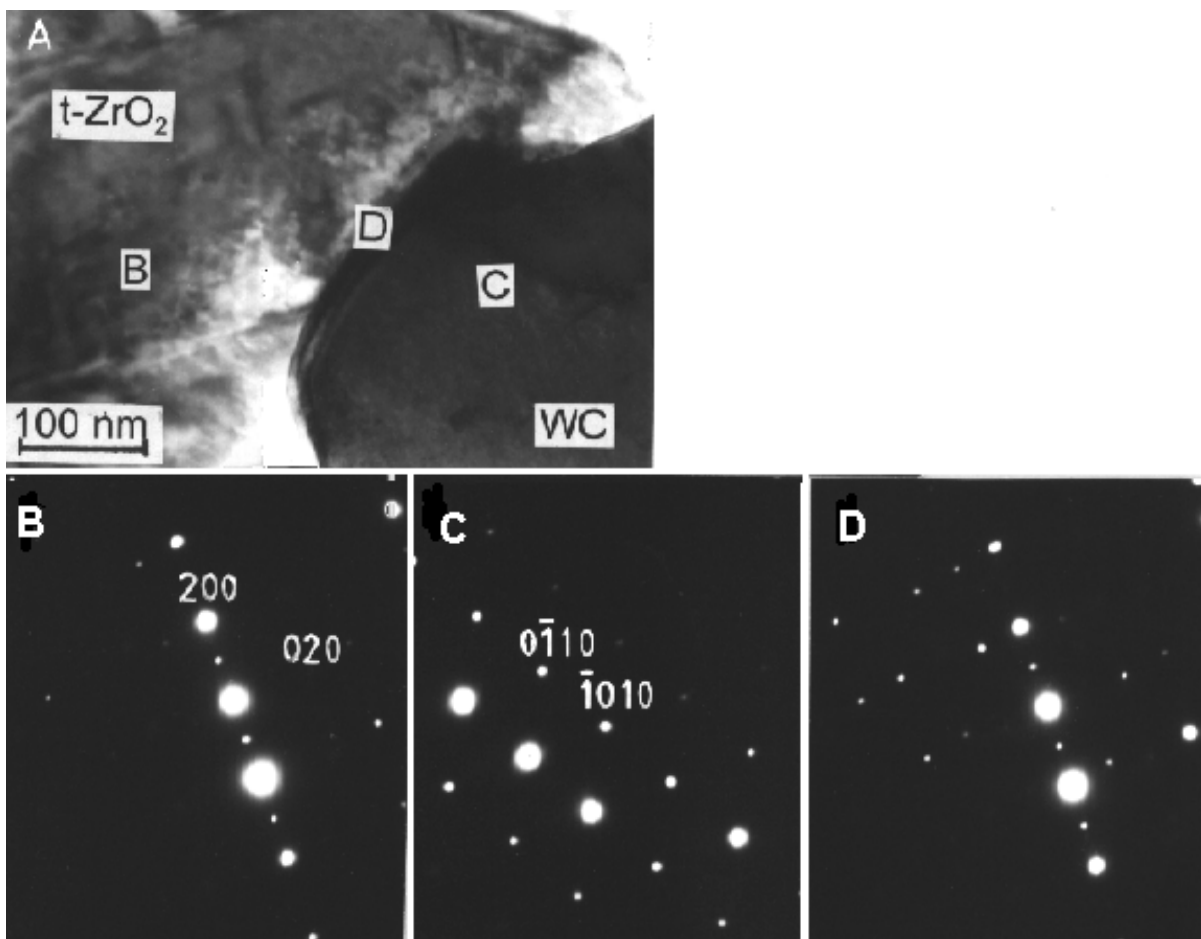


**Figure 15.** TEM micrograph of ZrO<sub>2</sub>/WC composite. A – BF image, B –SEAD from ZrO<sub>2</sub> grain, C– SEAD from WC grain, D – SEAD from the grain boundary region.

Similarly, in ZrO<sub>2</sub>/WC system crystallographic relationships were identified (Fig. 15) [36]:

$$[0001]\ \text{WC} \parallel [001]\ \text{tetragonal ZrO}_2 \quad (11)$$

$$[\bar{1}010] \text{ WC} \parallel [010] \text{ tetragonal ZrO}_2 \quad (12)$$

Furthermore, EBSD analysis made by Faryna et al. [37, 38] proved statistically that crystallographic correlation in investigated composite systems are not an unique property, but they are very often.

## 6. Mechanical properties

The basic mechanical properties of investigated materials were collected in Table 3. Both composites were well densified but it is worth to notice that there is about 1 % of difference between Al<sub>2</sub>O<sub>3</sub>/WC and ZrO<sub>2</sub>/WC composites. Zirconia matrix and zirconia-basing material is almost fully dense. Alumina-basing composite has “only” 98.8 % of theoretical density and is 0.5 % worse densified than alumina matrix. This difference is not much but certainly influence observed bending strength test results.

It is characteristic that Al<sub>2</sub>O<sub>3</sub>/WC material has lower bending strength than “pure” matrix material. Different effect is observed for ZrO<sub>2</sub>/WC composite. The mean value of the bending strength of ZrO<sub>2</sub>/WC is similar to that registered for zirconia matrix. But the highest strength value registered during tests was over 10% higher than that measured for zirconia matrix. This fact showed that there is a potential of strength improvement in this system.

It is not surprise that hardness of composites is higher than that measured for matrices. Spectacular is the increase of the fracture toughness. In both investigated composite systems  $K_{Ic}$  increased more than 50 % when compared with the suitable matrix.

Material	Relative density, $Q_{wzgl.}$ , %	Vickers hardness, $HV$ , GPa	Young's modulus, $E$ , GPa	Fracture toughness, $K_{Ic}$ , MPam <sup>0.5</sup>	Bending strength – the mean value, $\sigma$ , MPa	Bending strength – maximum value, $\sigma_{max}$ , MPa	Weibull parameter, $m$
Alumina	99.3 ± 0.1	17.0 ± 1.2	379 ± 6	3.6 ± 0.3	600 ± 120	780	6
Alumina/10vol.% WC	98.8 ± 0.1	18.7 ± 0.8	394 ± 7	5.5 ± 0.7	450 ± 45	550	12
Zirconia s.s.	99.5 ± 0.1	14.0 ± 0.5	209 ± 5	5.0 ± 0.5	1150 ± 75	1250	18
Zirconia/10vol.% WC	99.7 ± 0.1	17.0 ± 0.9	232 ± 6	8.0 ± 1.0	1100 ± 130	1380	7

± denotes the confidence interval on the 0.95 confidence level (for  $Q$ ,  $HV$  and  $K_{Ic}$  measurements);

± denotes the standard deviation of the mean value of 40 results of measurements (for  $\sigma$  measurements).

**Table 3.** Mechanical properties of the matrices and composites.

Experiments of subcritical crack propagation performed using Double Torsion method (DT) [39- 41] showed that composites were much more resistant for this disadvantageous

phenomenon. Such experiments were previously conducted for alumina and zirconia materials [42, 43] but not for composites containing tungsten carbide particles. Results of performed investigations (see Fig. 16) showed that the threshold value of  $K_I$  coefficient in both composite systems significantly increased. In  $\text{Al}_2\text{O}_3/\text{WC}$  material the threshold  $K_I$  value was  $\sim 4.0 \text{ MPam}^{-0.5}$  (compared with  $2.6 \text{ MPam}^{-0.5}$  for alumina). In  $\text{ZrO}_2/\text{WC}$  material the threshold  $K_I$  value was  $\sim 4.4 \text{ MPam}^{-0.5}$  (compared with  $3.6 \text{ MPam}^{-0.5}$  for zirconia). The most probably reason of such behaviour was the residual stresses state in dense sintered composite bodies. Distribution of these stresses around composite hindered breaking of atomic bonds on the tip of flaws presented in composites.

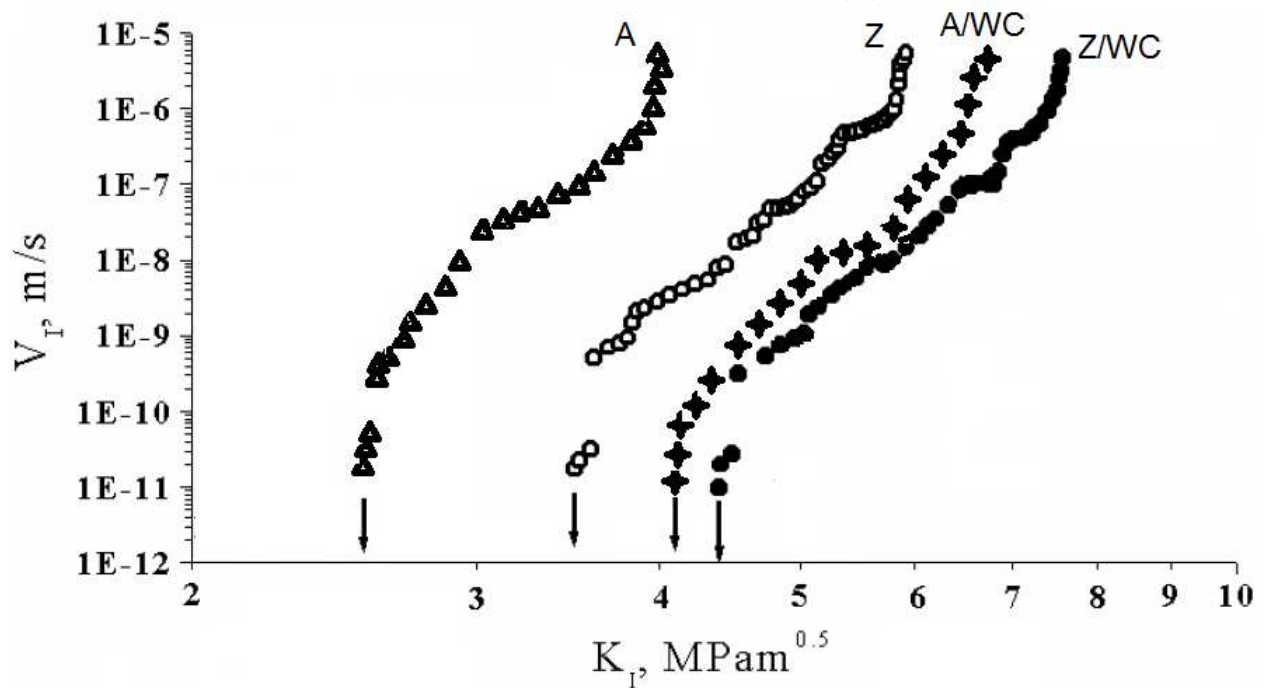


**Figure 16.** The crack velocity  $V_I$  vs. stress intensity factor  $K_I$ . A, Z, A/WC, Z/WC – stand for alumina, zirconia, alumina/WC composite and Zirconia/WC composite, relatively.

## 7. Wear resistance

One of the most important field of structural ceramic application is using them as a part of devices resistant for abrasive wear. From this point of view it is important how the material behaves at different working conditions (the range of loads) and environments (the presence of humidity). The oxide matrices are sensitive for water presence in environment. Even under low load rate it can cause the subcritical crack growth [42 - 45]. If the load are serious, degradation of the oxide matrices in the presence of water could be very significant.

The chapter presents the results of investigation on wear of alumina and zirconia-basing composites by hard abrasive particles in different environments. The results of two tests (The Dry Sand Test and the Miller Test in pulp) were compared. As an abrasive medium coarse silicon carbide grains were used in both cases.

The type of Dry Sand Test based on ASTM test [46], which indicates wear susceptibility of material for wear during abrasive action of hard particles without any lubricant. The test duration was 2000 rotation of the wheel.

The Miller Test based on ASTM test [47] allows to determine of SAR (Slurry Abrasion Response) number during the wear in slurry. The test duration was 6 hours. In both test the low value of test result means the better material behaviour.

Results of performed wear tests were collected in Table 4.

Material	Miller Test, SAR number,	Dry Sand Test, wear rate in mm <sup>3</sup>
Alumina	163.51	55.17
Alumina/10vol.% WC	9.57	9.57
Zirconia s.s.	9.45	15.71
Zirconia/10vol.% WC	7.41	11.46

**Table 4.** Results of performed wear tests.

The results showed difference in wear mechanisms between tests conducted in dry and wet environments for composites with two matrices:  $\alpha$ -alumina and tetragonal zirconia. Figures 17 and 18 collect SEM images of worn surfaces after the Dry Sand Test and the Miller Test. The fundamental difference visible at these figures, especially for alumina phase, is the presence of intensive grain boundary etching during work in wet environment. It could lead even to the whole grain scouring from the sintered bodies. During the Dry Sand Test the dominant wear mechanism consists in grains fracture. The presence of hard WC particles in both investigated oxide matrices limits the wear rates.

The worn surface profilographic analysis (see Table 5) allows to establish that second phase particle addition modifies alumina microstructure significantly. Alumina-basing composite surface after both tests were much more smooth, than the pure matrix surface. It proved that the dominant wear mechanisms were significantly limited.

Comparing the pure zirconia and zirconia-basing composite materials is visible that composite surface roughness is higher. Anyway, the wear rates for zirconia-basing composites were lower than for pure zirconia material.

Wear properties of both (alumina or zirconia) composite types are distinctly different in spite of wear environment.

Conducted tests established that incorporation of second phase grains into alumina matrix influences wear properties changes in high scale. Changes observed for zirconia based composites are not so spectacular but still significant.

Results of performed wear tests suggest that investigated materials are predicted to work at different environments. The wear resistant parts for work at wet environments seem to be

the best area of application for zirconia composites. Alumina based materials show the best properties during dry abrasion.

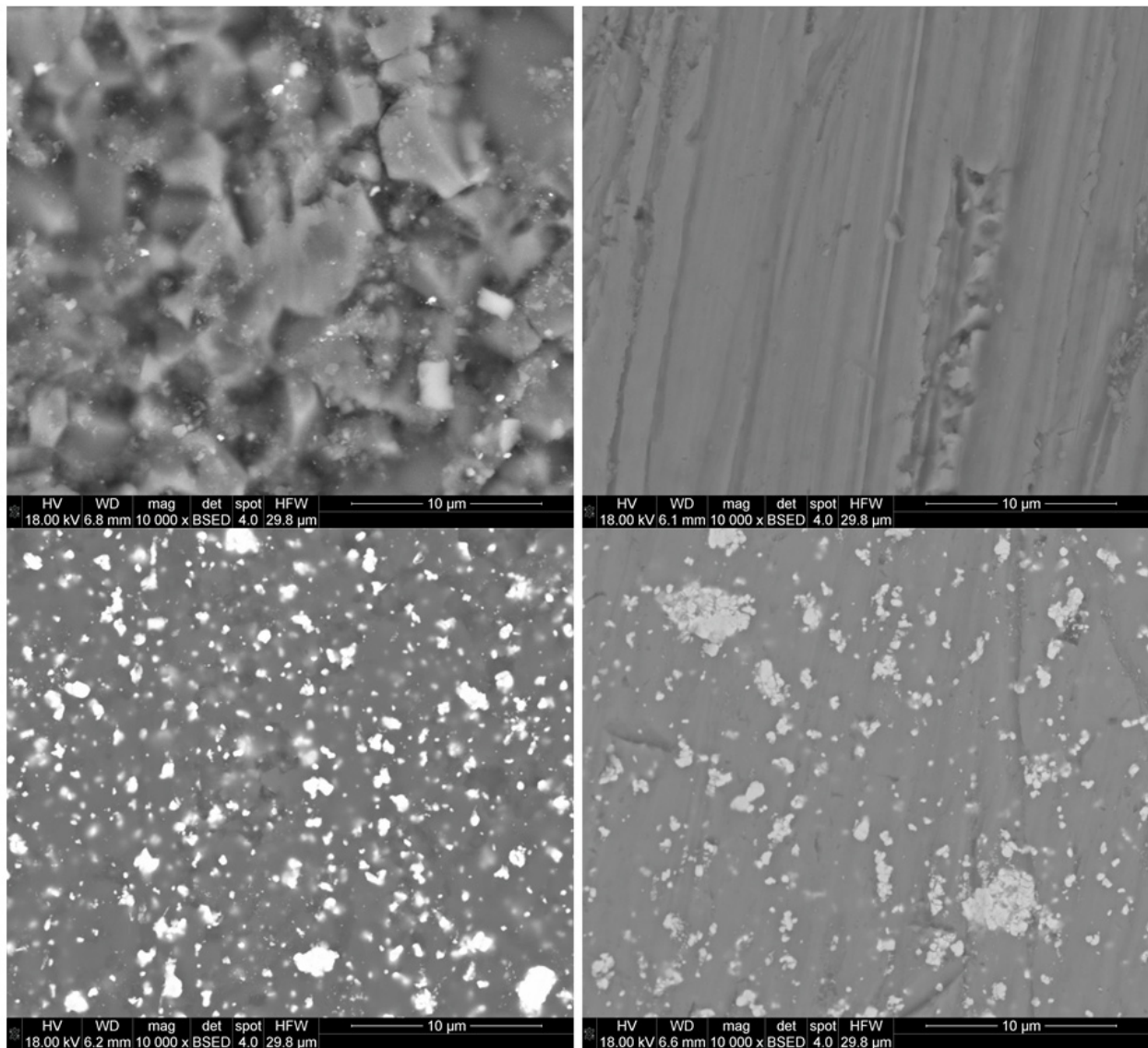


**Figure 17.** A typical microstructures of worn surfaces after Dry Sand Test; alumina (left top), zirconia s. s. (right top), alumina/10vol.% WC (left bottom), zirconia/10vol.% WC (right bottom).

Material	Miller Test	Dry Sand Test
	R <sub>a</sub> [μm]	R <sub>a</sub> [μm]
Alumina	0,66 ±0,11	1,02 ±0,05
Alumina/10vol.% WC	0,28 ±0,05	0,50 ±0,02
Zirconia s.s.	0,61 ±0,03	0,71 ±0,04
Zirconia/10vol.% WC	1,00 ±0,14	1,12 ±0,09

± denotes of the standard deviation of 5 measurements

**Table 5.** Profilographic parameter R<sub>a</sub> of material surfaces worn during wear tests.

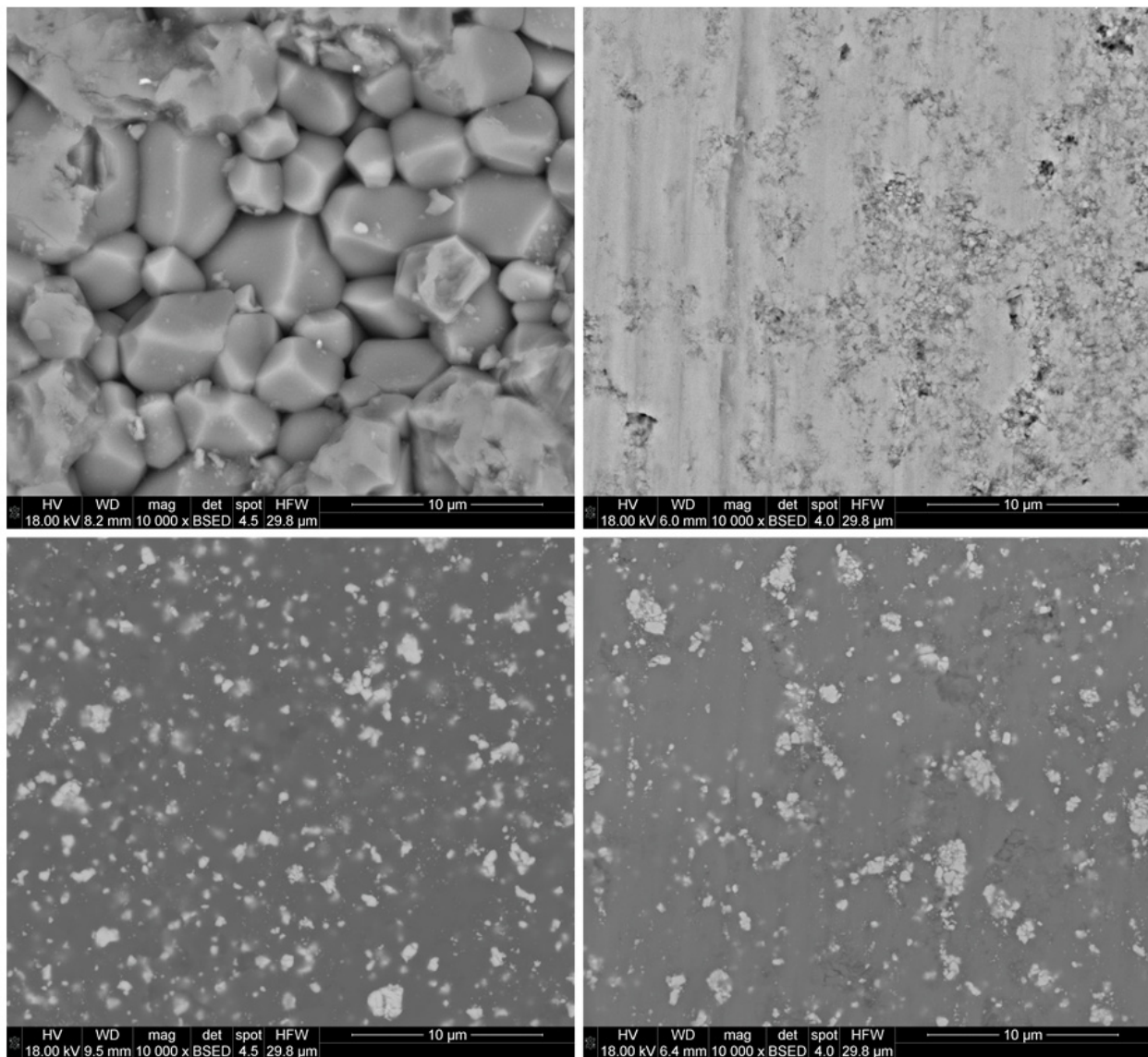


**Figure 18.** A typical microstructures of worn surfaces after Miller Test; alumina (left top), zirconia s. s. (right top), alumina/10vol.% WC (left bottom), zirconia/10vol.% WC (right bottom).

## 8. Summary

Selected information about properties of composite materials basing on alumina or zirconia matrices containing dispersed tungsten carbide inclusions presented in this chapter indicated that these materials have potential to be widely used as a structural material.

Properties improvement in these composites is not only an effect of introducing an additional toughening mechanisms connected with crack path/inclusion interacting (crack deflection, crack branching, crack bridging), but also relatively strong interphase grain boundaries confirmed by the unique phenomenon of privileged crystallographic correlation of oxide and carbide phases.

Their very good properties are manifest in applications connected with intensive wear risks, especially in the presence of loose, hard particles. Spectacular improvement was also observed in prolonged applications at conditions under stresses much lower than critical at wet or high humid environments.

## Author details

Zbigniew Pędzich

AGH – University of Science and Technology, Krakow, Poland

## 9. References

- [1] Ding, Zh., Oberacker, R. and Thümler, F., Microstructure and mechanical properties of yttria stabilized tetragonal zirconia polycrystals (Y-TZP) containing dispersed silicon carbide particles. *J. Europ. Ceram. Soc.* 1993; 12(5) 377-383.
- [2] Nawa M., Yamazaki K., Sekino T., Niihara K., A New Type of Nanocomposite in Tetragonal Zirconia Polycrystal – Molybdenum System. *Materials Letters.* 1994; 20 299-304.
- [3] Poorteman M., Descamps P., Cambier F., Leriche E., Thierry B., Hot Isostatic Pressing of SiC-Platelets/Y-TZP. *J. Europ. Ceram. Soc.* 1993; 12 103-109.
- [4] Claussen N., Weisskopf K.L. and Ruhle M., Tetragonal zirconia polycrystals reinforced with SiC whiskers. *J. Am. Ceram. Soc.* 1986; 68 288-292.
- [5] Lin G.Y., Lei T. C., Wang S. X. and Zhou Y., Microstructure and mechanical properties of SiC whisker reinforced ZrO<sub>2</sub> (2 mol% Y<sub>2</sub>O<sub>3</sub>) based composites. *Ceramics International* 1996; 22 199-205.
- [6] Wahi R.P. and Ilschner B., Fracture behavior of composites based on Al<sub>2</sub>O<sub>3</sub>-TiC. *Mater. Sci. Eng.* 1980; 15 875-885.
- [7] Tieggs T.N. and Becher P.F., Sintered Al<sub>2</sub>O<sub>3</sub>-SiC Composites. *Am. Ceram. Soc. Bull.* 1987; 66(2) 339-342.
- [8] Niihara K., Nakahira A., Sasaki G. and Hirabayashi M., Development of strong Al<sub>2</sub>O<sub>3</sub>/SiC composites. *MRS Znt. Mtg. on Adv. Mater. Vol. 4* 1989; 129-134.
- [9] Stadlbauer W., Kladnig W. and Gritzner G., Al<sub>2</sub>O<sub>3</sub>/TiB<sub>2</sub> composite ceramics. *J. Mater. Sci. Lett.* 1989; 81217-1220.
- [10] Borsa C.E., Jiao S., Todd R.I. and Brook R.J., Processing and properties of Al<sub>2</sub>O<sub>3</sub>/SiC nanocomposites. *J. Microscopy.* 1994; 177 305-312.
- [11] Breval E., Dodds, G. and Pantano C.G., Properties and microstructure of Ni-alumina composite materials prepared by the sol/gel method. *Mater. Res. Bull.* 1985; 20 1191-1205.
- [12] Sekino T., Nakahira A. and Niihara K., Relationship between microstructure and high-temperature mechanical properties for Al<sub>2</sub>O<sub>3</sub>/W nanocomposites. *Trans. Mater. Res. Soc. Jpn.* 1994; 16B, 1513-1516.
- [13] Vleugeus J. and Van Der Biest O., ZrO<sub>2</sub>-TiX Composites. *Key Engineering Materials, Vols. 132-136, Trans Tech Publications, Switzerland, 1997; 2064-2067.*

- [14] Changxia L, Jianhua Z., Xihua Z., Junlong S., Fabrication of  $\text{Al}_2\text{O}_3/\text{TiB}_2/\text{AlN}/\text{TiN}$  and  $\text{Al}_2\text{O}_3/\text{TiC}/\text{AlN}$  composites. *Materials Science and Engineering A*. 2003; 99(1-3) 321-324.
- [15] Acchara W., Silva Y.B.S, Cairoc C.A., Mechanical properties of hot-pressed  $\text{ZrO}_2$  reinforced with (W,Ti)C and  $\text{Al}_2\text{O}_3$  additions. *Materials Science and Engineering A*. 2010; 527 480-484.
- [16] Pędzich Z., Haberko K., Babiarz J., Faryna M., TZP - chromium oxide and chromium carbide composites. *J. Europ. Ceram. Soc.* 1998; 18(13) 1939-1943.
- [17] Pędzich Z., Haberko K., Piekarczyk J., Faryna M., Lityńska L., Zirconia matrix - tungsten carbide particulate composites manufactured by hot-pressing technique. *Materials Letters*. 1998 36(7) 70-75.
- [18] Garvie R.C., Stabilization of the Tetragonal Structure in Zirconia Microcrystals. *J. Phys. Chem.* 1978; 82(2) 218-224.
- [19] Kontouros P., Petzow G., Defect Chemistry, Phase Stability and Properties of zirconia Polycrystals. In *Science and Technology of Zirconia V*. Technomic Publishing Co. Inc. Eds.: Badwall S.P.S., Bannister M.J., Hannink R.H.J. 1992.
- [20] Zhang Y., Xu G., Yan Z., Liao C. and Yan C. Nanocrystalline rare earth stabilized zirconia: solvothermal synthesis via heterogeneous nucleation-growth mechanism, and electrical properties. *J. Mater. Chem.* 2002;12 970-977
- [21] Barin I., Knacke O., *Thermochemical Properties of Inorganic Substances*. Springer-Verlag, Berlin. 1973
- [22] Haberko K., Pędzich Z., Piekarczyk J., Bućko M.M., Suchanek W., "Tetragonal Zirconia Polycrystals Under Reducing Conditions", *Proceedings of Third Euro-Ceramics*, vol. 1, Processing of Ceramics, Eds. P.Duran, J.F.Fernandez., Faenza Editrice Iberica S. L., Hiszpania, 1993; 967-972.
- [23] Niyomwas S., The Effect of Diluents on Synthesis of Alumina-Tungsten Carbide Composites by Self-Propagating High Temperature Synthesis Process, *Proceedings of Technology and Innovation for Sustainable Development International Conference (TISD2010)*, Faculty of Engineering, Khon Kaen University, Thailand, 4-6 March 2010, 1025-1029.
- [24] PTC – the Product Development Company, <http://www.ptc.com>
- [25] Pro/Mechanica – computer program user book (documentation)
- [26] Pędzich Z., The reliability of particulate composites in the TZP/WC system. *J. Europ. Ceram. Soc.* 2004; 24(12) 3427-3430.
- [27] Jiang D.T., Van der Biest O., Vleugels J.,  $\text{ZrO}_2$ -WC nanocomposites with superior properties, *J. Europ. Ceram. Soc.* 2007; 27 1247-1251.
- [28] Ünal N., Kern F., Övecoglu M.L., Gadow R., Influence of WC particles on the microstructural and mechanical properties of 3 mol%  $\text{Y}_2\text{O}_3$  stabilized  $\text{ZrO}_2$  matrix composites produced by hot pressing, *J. Europ. Ceram. Soc.* 2011; 31 2267-2275.
- [29] Preiss H., Meyer B. and Olschewski C., Preparation of molybdenum and tungsten carbides from solution derived precursors. *J. Mater. Sci.* 1998; 33(3) 713-722.
- [30] Kim J.C, Kim B.K., Synthesis of nanosized tungstencarbide powder by the chemical vapor condensation process. *Scripta Materialia*. 2004; 50(7) 969-972.

- [31] Rahaman M.N., De Jonghe L.C., Effect of rigid Inclusions on Sintering. Proceedings of First International Conference on Ceramic Powder Processing, Orlando FL. 1-4 November 1987.
- [32] Scherer G.W., Sintering with Rigid Inclusions. *J. Amer. Ceram. Soc.* 1987; 70(10) 719-725.
- [33] Weiser M.W., De Jonghe L.C., Inclusion size and Sintering of Composite Powders. *J. Amer. Ceram. Soc.* 1988; 71(3) C125-C127.
- [34] Zhao C., Vleugels J., Basu B., Van Der Biest O., High toughness Ce-TZP by sintering in an inert atmosphere, *Scripta Materialia*. 2000; 43 1015-1020.
- [35] Pędzich Z., Faryna M., Fracture and Crystallographic Phase Correlation in Alumina Based Particulate Composites, in *Fractography of Advanced Ceramics II - Key Engineering Materials Vol. 290*, Eds. Dusza J., Danzer R. and Morrell R. Trans Tech Publications, Switzerland, 2005; 142-148.
- [36] Faryna M., Bischoff E., Sztwiertnia K., Crystal orientation mapping applied to the Y-TZP/WC composite. *Microchimica Acta*. 2002; 135 55-59.
- [37] Sztwiertnia K., Faryna M., Sawina G., Misorientation characteristics of interphase boundaries in particulate Al<sub>2</sub>O<sub>3</sub>-based composites, *J. Europ. Ceram. Soc.* 2006; 26 2973-2978
- [38] Faryna M., TEM and EBSD comparative studies of oxide-carbide composites. *Material Chemistry and Physics*. 2003; 81 301-304.
- [39] Chevalier J., Saadaoui M., Olagnon C., Fantozzi G., Double-torsion testing a 3Y-TZP ceramic. *Ceramics International*. 1996;22 171-177.
- [40] Evans, A.G., A method for evaluating the time-dependent failure characteristics of brittle materials—and its application to polycrystalline alumina. *Journal of Materials Science*. 1972; 7(10) 1137-1146.
- [41] Williams D.P. and Evans A.G., A simple method for studying slow crack growth. *J. Testing and Evaluation*. 1973; 1 264-270.
- [42] Chevalier, J., Olagnon, C. and Fantozzi, G., Subcritical crack propagation in 3Y-TZP ceramics: static and cyclic Fatigue. *J. Am. Ceram. Soc.*, 1999, 82(11), 3129–3138.
- [43] Ebrahimi, M.E., Chevalier J. and Fantozzi G., Slow crack-growth behavior of alumina ceramics. *Journal of Materials Research*. 1999; 15 142-147.
- [44] Morita Y., Nakata K., Kim Y.H., Sekino T., Niihara K., Ikeuchi K., Wear properties of alumina/zirconia composite ceramics for joint prostheses measured with an end-face apparatus, *Biomed Mater Eng*. 2004; 14(3) 263-270.
- [45] Pędzich Z., The Abrasive Wear of Alumina Matrix Particulate Composites at Different Environments of Work. In *Advanced Materials and Processing IV*, Eds. Zhang D. , Pickering K., Gabbitas B., Cao P., Langdon A., Torrens R. and Verbeek J. Trans Tech Publications, Switzerland, 2007; 29-30 283-286.
- [46] ASTM 65 - 94 Test Method for Measuring Abrasion Using the Dry Sand/Rubber Wheel Apparatus
- [47] ASTM G 75 - 95 Test Method for Determination of Slurry Abrasivity (Miller Number) and Slurry Abrasion Response of Materials (SAR Number).